



**HAL**  
open science

## Spatial arrangement of casein micelles and whey protein aggregate in acid gels: Insight on mechanisms

Robi Andoyo, Fanny Guyomarc'H, Agnès Burel, Marie-Hélène Famelart

### ► To cite this version:

Robi Andoyo, Fanny Guyomarc'H, Agnès Burel, Marie-Hélène Famelart. Spatial arrangement of casein micelles and whey protein aggregate in acid gels: Insight on mechanisms. *Food Hydrocolloids*, 2015, 51, pp.118-128. 10.1016/j.foodhyd.2015.04.031 . hal-01209825

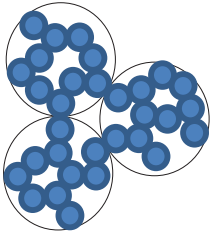
**HAL Id: hal-01209825**

**<https://hal.science/hal-01209825>**

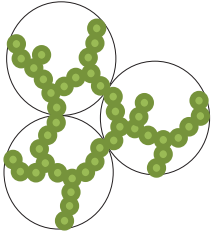
Submitted on 12 Nov 2015

**HAL** is a multi-disciplinary open access archive for the deposit and dissemination of scientific research documents, whether they are published or not. The documents may come from teaching and research institutions in France or abroad, or from public or private research centers.

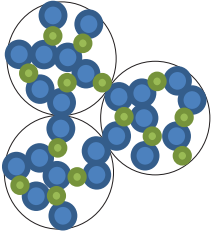
L'archive ouverte pluridisciplinaire **HAL**, est destinée au dépôt et à la diffusion de documents scientifiques de niveau recherche, publiés ou non, émanant des établissements d'enseignement et de recherche français ou étrangers, des laboratoires publics ou privés.



**Casein micelles**



**Whey protein aggregates**



**Mixture**

# Spatial arrangement of casein micelles and whey protein

## aggregate in acid gels: Insight on mechanisms

Robi ANDOYO<sup>abc</sup>, Fanny GUYOMARC'H<sup>ab</sup>, Agnes BUREL<sup>d</sup>,

Marie-Hélène FAMELART<sup>ab,\*</sup>

<sup>a</sup>INRA, UMR1253, Science et Technologie du Lait et de l'Œuf, 65 rue de St Briec, F-35  
042 Rennes cedex, France

<sup>b</sup>AGROCAMPUS OUEST, UMR 1253, Science et Technologie du Lait et de l'Œuf, 65  
rue de St Briec, F-35 042 Rennes cedex, France

<sup>c</sup>Faculty of Agriculture Industrial Technology, Padjadjaran University, Indonesia

<sup>d</sup>Université de Rennes 1 France, Microscopy Rennes Imaging Center of SFR BIOSIT. 2  
Avenue du professeur Léon Bernard, 35043 Rennes cedex, France

\* Corresponding author; Tel: +33.223.48.53.43; Fax: +33.223.48.53.50; email address: [marie-helene.famelart@rennes.inra.fr](mailto:marie-helene.famelart@rennes.inra.fr)

Keywords: whey proteins, casein micelles, acid gel, rheology, microstructure, fractal analysis

**Running title:** mechanism of acid gelation of model acid gels

### ABSTRACT

Skim milk used for the yoghurt manufacture contains 2 main colloidal particles, the native micellar casein (NMC) and the heat-induced whey protein aggregates (WPA). The aim of this study was to understand how these 2 colloids organize in space to form binary acid gels. While acid milk gels were considered homogeneous for scales typically above  $\sim 10 \mu\text{m}$ , shorter length scales were examined to investigate the early stages of particle aggregation. The NMC and WPA were dispersed in milk permeate at different protein concentrations,

23 separately or in an 80/20 w/w mixture (MIX). Acidification was performed at 35 °C with  
24 glucono- $\delta$ -lactone to achieve a final pH at  $\sim$  4.5 in 6 h. Acid gelation was studied by  
25 rheology, while the microstructure of the gels at pH 4.5 was studied by confocal scanning  
26 laser microscopy and transmission electron microscopy (TEM). Using Shih et al.'s (1990)  
27 model on the rheological data, it seemed that aggregation in the NMC and MIX mixtures was  
28 driven by the casein micelles and therefore differed from that of the WPA suspension. The  
29 different organizations were confirmed using image analysis of confocal or TEM images. The  
30 differences in gel formation were discussed in terms of the different interactive properties of  
31 the surface of these 2 colloids, together with their different internal structure.

## 32 1. Introduction

33 The protein components of milk contain two types of colloidal particles, namely caseins  
34 and whey proteins. Caseins assemble as colloidal particles having diameter of ~ 200 nm  
35 called casein micelles that occupy a volume fraction  $\Phi$  of ~0.1 in skim milk (Holt, 1992).  
36 These micelles contain several thousands of  $\alpha_{s1}$ ,  $\alpha_{s2}$ ,  $\beta$ - and  $\kappa$ -casein molecules as well as  
37 minerals, essentially in the form of colloidal calcium phosphate (CCP) (de Kruif, 1999; Fox &  
38 Brodkorb, 2008). CCP ionic bridges and hydrophobic interactions are responsible for the  
39 integrity of the micelles (Dalglish, 2011; Horne, 1998). The  $\kappa$ -casein, located at the surface  
40 of casein micelles, contributes to their stability through steric and electro-negative repulsion  
41 (de Kruif & Huppertz, 2012; Panouillé, Durand, Nicolai, Larquet, & Boisset, 2005). During  
42 acidification, the hairy layer of  $\kappa$ -casein collapses at pH ~6.0 while the electrostatic repulsion  
43 decreases as the casein micelles reach their isoelectric pH (pI) of about 4.6, where  
44 destabilization eventually occurs (Lucey & Singh, 1998).

45 Heating of milk at ~60°C or above makes the whey protein unfold and irreversibly  
46 denature, yielding to the formation of heat-induced whey protein aggregates (WPA), built  
47 through thiol oxidation, thiol/disulphide exchange and hydrophobic interactions (Donato &  
48 Guyomarc'h, 2009; Parris, Anema, Singh, & Creamer, 1993; Parris, Hollar, Hsieh, &  
49 Cockley, 1997; Singh & Creamer, 1991). Upon acidification, these aggregates accelerate the  
50 destabilization of casein micelles due to their higher surface hydrophobicity and slightly  
51 higher pI (Guyomarc'h, Renan, Chatriot, Gamarre, & Famelart, 2007; Morand, Dekkari,  
52 Guyomarc'h, & Famelart, 2012; Morand, Guyomarc'h, Legland, & Famelart, 2012).  
53 Aggregates are also thought to act as bridges between the casein micelles and to strengthen  
54 the acid gel network (Alexander, Corredig, & Dalglish, 2006; Famelart, Tomazewski, Piot,  
55 & Pezennec, 2004; Guyomarc'h, Queguiner, Law, Horne, & Dalglish, 2003). Andoyo et al.  
56 (2014) showed that the coating of only ~8% of the casein micelle surface by WPA produced

57 gels with significantly higher storage modulus values ( $G'$ ) than those made of casein only.  
58 Therefore, the interaction between these particles and the mechanism of their assembly is  
59 likely to direct the structural and mechanical properties of the acid gel. However, the  
60 mechanisms that drive this interaction need to be further investigated.

61 Acid milk gels are particulate gels that appear as a porous, homogeneous material at  
62 length scales above tens of  $\mu\text{m}$ . Various models have been proposed to describe their  
63 formation and structure; namely the adhesive sphere, the percolation and the fractal models  
64 (Horne, 1999). While the adhesive sphere theory tells whether particles are stable in certain  
65 environmental conditions, the percolation theory informs on the dynamics of gel formation  
66 from the point when diffusion in the bulk is restricted by the growth of flocs of aggregated  
67 particles. In other words, the former rather focuses on the initial stages of aggregation at the  
68 particle's length scale, while the latter rather applies from the gelation point onward and at  
69 length scales of tens of  $\mu\text{m}$  and beyond. At intermediate length scales, typically 0.1-5  $\mu\text{m}$ ,  
70 Bremer et al. (1989) applied the self-similarity concept to describe the acid gelation of casein  
71 particles. Therefore, it is proposed that the fractal model may describe particle aggregation in  
72 a mixture of both particles, from the point when acidification renders the particles reactive (de  
73 Kruif, 1999) to the point when clusters have grown enough to come in close contact,  
74 interpenetrate and percolate. To the authors' knowledge, little research has yet been  
75 undertaken that could help model early flocculation in binary colloidal suspensions of casein  
76 micelles and whey protein aggregates, where the two particles differ in size and reactivity  
77 (Andoyo et al., 2014; Nair, Dalgleish, & Corredig, 2013).

78 Various scaling models have been developed and used in protein and colloidal gels to infer  
79 information on the mechanism of assembly of particles and on the structure of the final  
80 particulate gel network from rheological data or image analysis (Alting, Hamer, de Kruif, &  
81 Visschers, 2003; Bremer, Bijsterbosch, Schrijvers, Van Vliet, & Walstra, 1990; Buscall,

82 Mills, Goodwin, & Lawson, 1988; Marangoni, Barbut, McGauley, Marcone, & Narine, 2000;  
83 Shih, Shih, Kim, Liu, & Aksay, 1990; Sonntag & Russel, 1987). In this approach, the fractal  
84 dimension ( $D_f$ ) is used to describe the occupancy of the structure in the volume of the gel,  
85 while the scaling behavior can give insight on the mechanism of assembly of the particles.  
86 The model developed by Shih et al. (1990) proposes an estimation of the fractal dimension  
87 ( $D_f$ ) based on the rheological properties of the gel system. This model calculates the  $D_f$  values  
88 using  $G'$  and the strain at limit of linearity ( $\gamma_0$ ) of gels produced at different protein  
89 concentrations ( $C$ ). Furthermore, this concept gives insight to the building of the gel, since  
90 aggregation can follow two distinct pathways indicated by the either positive or negative  
91 slope of  $\log(\gamma_0)$  as a function of  $\log(C)$ .

92 In this study, the gelation properties, aggregation behavior and the fractal dimension of the  
93 flocs of casein micelles, of the WPA and of their mixture in acid gel were investigated, in  
94 order to better understand the mechanisms of formation of dairy acid gels. Since milk is a  
95 rather crowded system, diffusion is probably rapidly restricted upon cluster growth and fractal  
96 structures may be searched only locally. For that reason, microscopies were also used to  
97 support the rheological approach.

## 98 **2. Materials and Methods**

### 99 **2.1. Materials**

100 A commercial whey protein isolate (WPI) (Prolacta 95, Lactalis Ingredients, Bourgbarré,  
101 France) was used as the source of protein in this study. The protein content of the WPI  
102 powder is  $\sim 939 \text{ g kg}^{-1}$  dry matters. Protein content was determined by Kjeldahl method  
103 (conversion factor 6.38).

104 Native micellar casein (NMC) was prepared by microfiltration of raw skim milk,  
105 diafiltration and spray-drying as described by Schuck et al. (1994). Skim milk microfiltration

106 also yielded a whey protein permeate that was further ultra-filtered to produce milk  
107 ultrafiltration permeate (MUF). The MUF was stored at 5°C after addition of 0.2 g L<sup>-1</sup> sodium  
108 azide (NaN<sub>3</sub>). All other reagents were of analytical grade.

## 109 *2.2 . Preparation of the model systems*

110 WPA was produced by heating an aqueous WPI solution at total protein concentration of  
111 90 g kg<sup>-1</sup> and pH 7.5 at 68.5 °C for 2 h as described by Vasbinder, van de Velde and de Kruif  
112 (2004) and as used in Andoyo et al. (2014). The protein content of the resulting WPA  
113 suspension was determined spectrophotometrically using absorbance at 280 nm and an  
114 experimental extinction coefficient value of 1.2244 L g<sup>-1</sup> cm<sup>-1</sup> (Morand, Guyomarc'h,  
115 Pezennec, & Famelart, 2011). WPA was then standardized at 70 g kg<sup>-1</sup> total protein using  
116 MUF, extensively dialyzed (6-8 molecular-weight cut-off Spectra Por membrane) against  
117 commercial ultra-high temperature (UHT) skim milk to fully replace the solvent phase by  
118 MUF, then diluted again with MUF to reach concentrations (C) ranging 14 g kg<sup>-1</sup> to 62 g kg<sup>-1</sup>.  
119 Considering a voluminosity of 5.512 mL g<sup>-1</sup> for the WPA particles as measured at 20°C and  
120 pH 6.6 (Andoyo et al., 2014), the corresponding volume fractions ranged from 8 to 35% (v/v).  
121 This value of the volume fraction is only a rough estimate as we have no idea of the changes  
122 in voluminosity of WPA with temperature and pH.

123 A mother suspension of NMC at total protein concentration of 105 g kg<sup>-1</sup> was produced by  
124 gradually dispersing the required amount of NMC powder in MUF at 40°C with gentle  
125 stirring for 4 hours. The suspension was stored overnight at 4°C for complete hydration  
126 before further processing. NMC suspension at different total protein concentrations were  
127 prepared by diluting mother suspension with MUF. Total protein concentration of NMC  
128 ranged from 42g kg<sup>-1</sup> to 98g kg<sup>-1</sup>. Considering a voluminosity of 4.752 mL g<sup>-1</sup> for the NMC  
129 particles as measured at 20°C and pH 6.6 (Andoyo et al., 2014), a 10% decrease of the  
130 voluminosity with the increase in temperature from 20 to 35°C (Noebel, Weidendorfer, &

131 Hinrichs, 2012) and a 4% and 32% decrease in voluminosity with the decrease in pH from 6.6  
132 to 5.6 or 6.6 to 4.8, respectively (van Hooydonk, Hagedoorn, & Boerrigter, 1986), the  
133 corresponding volume fractions ranged approximately from 12 to 42% (v/v). The values of  
134 pH 5.6 and 4.8 are the respective pH of gelation of the suspensions at high and low  
135 concentration where the volume fraction has to be calculated. Using the same method, the  
136 volume fractions for the MIX systems were 6 to 37%.

137 Mother mixtures of NMC and WPA at 90 g kg<sup>-1</sup> and at the weight ratio of 80/20 were  
138 prepared by mixing appropriate amounts of each mother suspension. The mother mixture  
139 (MIX) suspension was then diluted with MUF to prepare mixtures ranging from 15 g kg<sup>-1</sup> to  
140 90 g kg<sup>-1</sup> total protein concentration (Table 1).

141 Systems will be called e.g. NMC45 or WPA15 or MIX60, the number representing their  
142 approximate total protein concentration in g kg<sup>-1</sup> (Table 1). All dairy systems were replicated  
143 at least two times and analyzed within one week.

### 144 ***2.3. Characterization of particles: Isoelectric pH***

145 The apparent isoelectric pH (pI) of the WPA and NMC were determined using  
146 interpolation to 0 of the experimental measurement of the electrophoretic mobility (in  $\mu\text{m}$   
147  $\text{cm V}^{-1} \text{s}^{-1}$ ), while the pH of the MUF was varied from 2.5 to 6.5 using HCl. The  
148 electrophoretic mobility was measured at 50 V and at 20°C on a Zetasizer nano ZS  
149 equipment ( $\lambda = 633 \text{ nm}$ , Malvern Instruments, Orsay, France). Colloidal suspensions were  
150 diluted at least 1:10 v/v in the MUF (dielectric constant 80.4, viscosity 1.1454 mPas,  
151 refractive index 1.337). This method yields lower apparent pI values (by ~0.2 pH units) than  
152 those obtained with MUF extracted from acidified skim milk (Guyomarc'h et al., 2007) or  
153 acidified MUF with added calcium (Morand et al., 2011), where the solubilization of CCP is  
154 taken into account. The resulting values were used only for comparison.

## 155 **2.4. Rheological measurements**

156 The WPA, NMC and MIX suspensions at different concentrations were equilibrated at  
157 35°C then acidified at this temperature using addition of glucono- $\delta$ -lactone (GDL) as to  
158 achieve a final pH value of 4.5 within 6 h (See concentrations of GDL used in Table 1).

159 Formation of the gels was monitored through the measurement of the storage modulus,  $G'$   
160 (in Pa), upon acidification at 35° C using an AR2000 rheometer (TA Instruments,  
161 Guyancourt, France) equipped with a cone-plane geometry (diameter 6 cm and cone angle 4°)  
162 using the oscillatory mode at a frequency of 1 Hz and 0.1% strain. The GDL was added to the  
163 sample, stirred for 1 min and the dairy system was then transferred to the rheometer. Low  
164 density paraffin oil was added around the sample to prevent evaporation. The gelation pH was  
165 defined as the moment when  $G' > 1$  Pa, while the storage modulus at pH 4.5 was considered  
166 to be the final  $G'$  at 35 °C ( $G'_{\max}$ ).

167 The gels at pH 4.5 were eventually subjected to a flow test. The strain,  $\gamma$  (dimensionless),  
168 was progressively increased at a constant rate of  $0.01\text{s}^{-1}$  until the gel broke. From this, the  
169 strain at the limit of linearity ( $\gamma_0$ ) or the end of the pure elastic behavior was obtained as the  
170 strain above which the slope of the stress versus strain curve decreased of 5% from its  
171 maximal value (insert Fig. 4). Each replicated system was measured twice.

## 172 **2.5. Microstructure of acid gels**

### 173 **2.5.1. Confocal laser scanning microscopy (CLSM)**

174 Samples for confocal image measurements were prepared as described by Andoyo et al.  
175 (2014). Briefly, the dairy system suspensions at 35°C were labeled using 0.06  $\mu\text{L}$  of  
176 rhodamine B isothiocyanate (RITC) per gram protein (from a 85 g  $\text{L}^{-1}$  RITC solution in  
177 dimethylsulfoxyde, Sigma-Aldrich, St Quentin Fallavier, France) and stirred for 15 min prior  
178 to the addition of GDL.

179 Immediately after GDL dispersion, ~60  $\mu\text{L}$  of the labeled sample was deposited on a  
180 conclave glass slide, covered with a cover slip, sealed with nail varnish and incubated at 35°C  
181 until pH 4.5. The slides were then imaged at 543 nm using a TE2000-E Nikon C1i inverted  
182 confocal laser scanning microscope (CLSM, Nikon, Champigny-sur-Marne, France). Each  
183 image was digitized in grey levels as a 512 x 512 pixel matrix (127.3 x 127.3  $\mu\text{m}^2$ ).

#### 184 2.5.2. *Transmission electron microscopy (TEM)*

185 The same procedure of microencapsulation as described in Andoyo et al. (2014) was  
186 employed for sample preparation of the gels. Briefly, gels were formed at 35°C in capillary  
187 tubes, fixed by glutaraldehyde-cacodylate and tannic acid-cacodylate solutions, dehydrated by  
188 ethanol, then embedded in an Epon-Araldite-DMP30 resin polymerized at 60°C. Ultra-thin  
189 sections (90 nm) of gels were cut in Leica UC6 ultra-microtome (Leica Microsystems,  
190 Vienna) and stained with 40 g L<sup>-1</sup> uranyl acetate for one hour.

191 The microencapsulation technique used in the current study has been used mainly for  
192 TEM of suspensions and emulsions (Kalab, 1981), but more rarely for acid gels like yoghurts.  
193 Most of the time, acid dairy gels are observed by scanning electron microscopy, with a  
194 glutaraldehyde fixation or by using a cryo-step. This encapsulation technique avoids problems  
195 for the sampling of soft gels and for the tendency of the gel to disperse into glutaraldehyde  
196 during fixation, but there is still problems arising from the fixation with glutaraldehyde,  
197 because of added intermolecular cross-links between proteins by the dialdehyde (Pawley,  
198 2010).

199 Sections were viewed with a JEOL 1400 transmission electron microscope (JEOL,  
200 Croissy-sur-Seine, France) supplied with GATAN Orius camera (Digital Micrograph  
201 software).

#### 202 2.6. *Determination of an apparent fractal dimension*

203 *2.6.1. From rheological measurement*

204 An apparent fractal dimension ( $D_f$ ) was evaluated from the slopes of the log ( $\gamma_0$ ) against  
 205 the log ( $C$ ) and log ( $G'$ ) against log ( $C$ ) based on the model of Shih et al. (1990) and using the  
 206 following equations when the slope of log ( $\gamma_0$ ) *versus* log ( $C$ ) is negative (equation 1-2) or  
 207 positive (equation 3-4) :

$$208 \quad G' \propto C^{(3+x)/(3-D_f)} \quad (1)$$

$$209 \quad \gamma_0 \propto C^{-(1+x)/(3-D_f)} \quad (2)$$

$$210 \quad G' \propto C^{(1)/(3-D_f)} \quad (3)$$

$$211 \quad \gamma_0 \propto C^{1/(3-D_f)} \quad (4)$$

212 With  $x$ , the backbone fractal dimension of the flocs, where the backbone is the fraction of the  
 213 fractal structure that is implied in stress transmission and hence, in the rheological response of  
 214 the structure (Genovese, 2012). Values from 1 to 1.3 are generally found for  $x$  (Shih et al.,  
 215 1990). The link regime of the particle assemblies can be identified by plotting log  $\gamma_0$  against  
 216 the log  $C$ . Shih et al. (1990) established that  $\gamma_0$  decreases with increasing  $C$  for a strong-link  
 217 assembly, while it increases for weak-link. For the weak-link regime, apparent  $D_f$  was only  
 218 calculated from  $G'$  values, while for the strong-link assembly, the apparent  $D_f$  values for  $x = 1$   
 219 and 1.3 were calculated, respectively, as done in previous works (Hagiwara, Kumagai, &  
 220 Nakamura, 1996; Ikeda, Foegeding, & Hagiwara, 1999; Shih et al., 1990).

221 *2.6.2 From confocal image analysis*

222 Images of the NMC, WPA and MIX gels were analysed with the public domain  
 223 software ImageJ 1.45s (<http://rsb.info.nih.gov/ij/>) and the fractal count plug-in  
 224 (<http://www.pvv.org/~perchrh/imagej/fractal.html>). The images were transformed into 8 bit  
 225 grey scale binary images of 512 x 512 pixels and were then thresholded using the method of

226 Pugnaroni et al. (2005). In this method, model systems before gelation were imaged as  
227 homogeneous images of the proteins and their mean grey level was calculated ( $GL_M$ ). Hence,  
228 if any pixel of an image of a gel has a grey level larger (i.e. whiter pixel) than the  $GL_M$ , it  
229 means that this pixel belongs to a structured place of the gel, namely to the network, and this  
230 pixel=1. Conversely if the pixel has a grey level lower than the  $GL_M$  (i.e. dark pixel), it  
231 belongs to the gel pores and the pixel=0. The apparent fractal dimension value ( $D_f$ ) was then  
232 measured on the converted image using the box counting method (Kaye, 1994) as a  
233 widespread technique used for gel microstructure analysis (Awad, Rogers, & Marangoni,  
234 2004; Bertoluzzo, Bertoluzzo, Luisetti, & Gatti, 1998; Bi, Li, Wang, & Adhikari, 2013; Eissa  
235 & Khan, 2005; Hagiwara, Kumagai, Matsunaga, & Nakamura, 1997; Kuhn, Cavallieri, & Da  
236 Cunha, 2010; Torres, Amigo Rubio, & Ipsen, 2012). The main principle of this method is to  
237 plot boxes of increasing sizes over an image and to count the number of boxes containing part  
238 of the protein network or flocs. The apparent fractal dimension value was calculated as the  
239 slope of the plot log number of boxes ( $N_\epsilon$ ) versus log size of the box ( $\epsilon$ ) or following this  
240 equation:

$$241 \quad D = - \frac{\text{Log} N_\epsilon}{\text{Log} \epsilon} \quad (5)$$

242 The slope ( $D$ ) represent the two-dimensional space fractal dimension, the 3-D  
243 apparent fractal dimension is calculated with the following equation:

$$244 \quad D_f = D + 1 \quad (6)$$

### 245 **2.6.3 From TEM image analysis**

246 TEM images of the NMC, WPA and MIX gels were analyzed with the ImageJ as for the  
247 confocal image analysis. The images were automatically thresholded using the ImageJ isodata  
248 algorithm where a threshold  $T$  is iteratively shifted toward the maximal grey value of the  
249 image until the mean grey level of pixels having a grey level  $< T$  is close to the mean grey

250 level of the pixels having a grey level  $>T$ . The software then determined the area and  
251 perimeter of objects or flocs for each cross section of the gel network in the image. The two-  
252 dimensional apparent fractal dimension ( $D$ ) for the flocs was calculated by regression analysis  
253 of the logarithm of their areas versus the logarithm of their corresponding perimeters (Dong,  
254 Wang, & Feng, 2011; Wang, Lu, Du, Shi, & Wang, 2009). The slope of the regression line is  
255 the value of  $D$ . The three-dimensional apparent fractal dimension ( $D_f$ ) was calculated as in  
256 equation 6.

### 257 3. Results and discussion

258 In the current study, it is postulated that varying the concentration of any of the 3 systems  
259 only changed the number of particles, without affecting the properties of the colloids, such as  
260 their size, charge and isoelectric pH.

#### 261 3.1. Acid gelation of the model systems

262 Using the different amounts of GDL as determined in Table 1, the kinetics of the pH  
263 versus acidification time were identical for all tested systems regardless of their total protein  
264 concentration or composition (results not shown). Noteworthy, what is important is the  
265 difference between the rate of the pH decrease and the rate of aggregation, which may affect  
266 gelation (Horne, 2001). Only when the aggregation rate can be shown to be identical for all  
267 systems or is much faster than the pH change, can the kinetics be fully ignored. Fig. 1A, 1C  
268 and 1E show the storage modulus ( $G'$ ) as a function of pH at different total protein  
269 concentrations of WPA, NMC or MIX systems, respectively. Increasing the total protein  
270 concentration in all systems resulted in an earlier gel formation, i.e. a higher pH of gelation,  
271 and led to a higher  $G'$  value at pH 4.5. The  $G'$  showed a steep increase from the point where  
272 the gels were formed ( $G' > 1$  Pa) then leveled off. However a  $G'$  plateau value was not reached  
273 within 6h of acidification (Van Vliet, Roefs, Zoon, & Walstra, 1989). A “G’ shoulder” was  
274 observed for protein concentrations above  $45 \text{ g kg}^{-1}$  for the NMC system and above  $15 \text{ g kg}^{-1}$

275 for the MIX system at pH 4.8-4.9 and then the  $G'$  value increased further until pH  $\sim$  4.5. Fig.  
276 1B, 1D and 1F show the value of  $\tan \delta$  as a function of pH of the model milk systems at  
277 different total protein concentrations. A higher value of  $\tan \delta$  indicates a more viscous-like  
278 behavior of the gel. For the WPA systems, the value of  $\tan \delta$  decreased as the gel formed, then  
279 leveled off towards a value of  $\sim$ 0.17. Meanwhile, for NMC and MIX systems, i.e. when casein  
280 micelles were present in the systems, the gels seemed to rearrange during acidification, as  
281 evidenced by the local maximum of  $\tan \delta$  at pH 4.9-5.1 (Fig. 1D and 1F). This maximum in  
282 the loss tangent was related to the shoulder seen in the  $G'$  curves (Fig. 1C,E) and is due to the  
283 solubilization of the CCP from the micelles resulting in a transient loosening of the gel  
284 network (Anema, 2009; Lucey, 2002; Ozcan-Yilsay, Lee, Horne, & Lucey, 2007). The values  
285 of the pH at the  $\tan \delta_{\max}$  are plotted as a function of the casein concentration (Fig. 2). We must  
286 point up that for the MIX series, the increase in casein concentration was also correlated with  
287 an increase in the whey protein aggregate concentration. It was clear that the pH at  $\tan \delta_{\max}$   
288 decreased with increasing casein concentrations for both systems from pH  $5.05 \pm 0.01$  to pH  
289  $4.89 \pm 0.01$ . From this general trend, the calculated value of the pH at the  $\tan \delta_{\max}$  could be  
290 described as a function of casein micelles concentration ( $\text{g kg}^{-1}$ ) derived from the equation of  
291 Debye-Huckel:

$$292 \quad \text{pH at the } \tan \delta_{\max} = A + \exp(-B * \text{square root}(C * \text{casein concentration})) \quad (7)$$

293 where A, B and C were constants, calculated by solver resolution that finds the optimal value  
294 of the constant. The increase in casein concentration in the NMC and MIX systems resulted in  
295 an increase in the ionic strength, hence in a decrease in the ionization of weak acids and in a  
296 small shift of CCP solubilization towards lower pH values (Famelart, Lepasant, Gaucheron,  
297 Le Graet, & Schuck, 1996).

298

299 **3.2. pH of gelation of the model milk systems**

300 Fig. 3A shows that the gels were formed at different pH values depending on the  
301 compositions of the model milk systems. When increasing from 15 to 70 g kg<sup>-1</sup> protein, the  
302 pH of gelation of the WPA system increased from 5.47 to 5.82. When increasing from 45 to  
303 105 g kg<sup>-1</sup> protein, the pH of gelation of the MNC system increased from 4.97 to 5.53, while  
304 when increasing from 15 to 90 g kg<sup>-1</sup> protein, the pH of gelation of the MIX system increased  
305 from 5.12 to 5.75. In all systems, the pH of gelation showed a linear correlation with the total  
306 protein concentration. This result was probably due to the increase in the number of particles  
307 and therefore, to the decrease of the inter-particle distance as the concentration increased. At  
308 all concentrations, the WPA-containing systems WPA and MIX both exhibited a significantly  
309 higher pH of gelation than the NMC system (Fig. 3A). In the current study, the apparent pI  
310 values of the WPA and NMC were found to be ~4.7 and ~4.4, respectively, which could  
311 partially explain the higher pH of gelation of WPA suspensions (Fig. 3B). These pI values  
312 were close to those found in other studies, namely 4.7 – 4.9 for whey protein aggregates  
313 (Jean, Renan, Famelart, & Guyomarc'h, 2006; Morand, Guyomarc'h, et al., 2012) and 4.2 -  
314 4.6 for the casein micelles (Guyomarc'h et al., 2007; Lucey & Singh, 1998). Whey protein  
315 aggregates also have a higher surface hydrophobicity as compared to casein micelles  
316 (Guyomarc'h et al., 2007; Jean et al., 2006; Morand, Dekkari, et al., 2012), which can  
317 overcome electrostatic repulsion and induced stabilization of the system at higher pH values  
318 (Famelart et al., 2004; Morand, Dekkari, et al., 2012; Morand, Guyomarc'h, et al., 2012). As a  
319 complement, Fig. 3A also shows calculated values of the pH of gelation based on the  
320 respective proportions of NMC and WPA in the MIX systems. The calculated values were far  
321 below those measured in the MIX system, indicating a cooperative interaction between the  
322 two types of particles (Andoyo et al., 2014). In the MIX systems, the association of WPA  
323 particles with the surface of casein micelles occurs before the onset of gelation (Alexander &

324 Dalgleish, 2005; Donato, Alexander, & Dalgleish, 2007; Donato, Guyomarc'h, Amiot, &  
325 Dalgleish, 2007; Guyomarc'h, Jemin, Le Tilly, Madec, & Famelart, 2009) and these  
326 associated WPA are thought to cover the surface of the micelles and progressively replace the  
327 surface properties of micelles by their own (Morand, Dekkari, et al., 2012; Morand,  
328 Guyomarc'h, et al., 2012; Morand et al., 2011). As a result, the pH of gelation of systems was  
329 dramatically increased when 20% WPA were present, in agreement with Andoyo et al.  
330 (2014).

### 331 **3.3. Rheological properties of the model milk systems at pH 4.5**

332 The double-log plot of the  $G'_{\max}$  of the gel as a function of the total protein concentration  
333 showed that increasing the protein concentration for the 3 systems led to higher  $G'_{\max}$  values  
334 with a power law dependence (Fig. 3C), probably as a result of the increasing number of  
335 particles as discussed above. When increasing from 15 to 70 g kg<sup>-1</sup> protein, the  $G'_{\max}$  value of  
336 the WPA system increased from  $1.06 \times 10^2$  to  $1.09 \times 10^5$  Pa. When increasing from 45 to 105  
337 g kg<sup>-1</sup> protein, the  $G'_{\max}$  value of the MNC system increased from  $2.5 \times 10^1$  to  $8.45 \times 10^3$  Pa,  
338 while when increasing from 15 to 90 g kg<sup>-1</sup> protein, the  $G'_{\max}$  value of the MIX system  
339 increased from  $1.6 \times 10^1$  to  $5.35 \times 10^3$  Pa. At 45 g kg<sup>-1</sup> (log45=1.65), Fig. 3C also showed that  
340 the MIX system exhibited more than 43 times higher  $G'_{\max}$  values than the NMC systems, in  
341 agreement with previous results (Andoyo et al., 2014). These authors explained that  
342 interaction of the WPA with the micelle surface led to the formation of earlier, more  
343 connected and stronger acid gels. However, Fig. 3C shows that such a significant effect of the  
344 presence of WPA in the MIX systems on the  $G'_{\max}$  was only observed at protein concentration  
345 less than 90 g kg<sup>-1</sup> (log 90=1.95). Indeed, the  $G'_{\max}$  of the NMC systems increased with  
346 concentration at a higher rate than that of the MIX systems (Fig. 3C). This could be due to  
347 differences in the dimensions or density of the casein micelles or flocs of micelles in either

348 the NMC or the MIX systems, as evidenced by TEM micrographs (Fig. 5), as discussed  
349 below.

350 When comparing the three different model milk systems, Fig. 3C furthermore shows that  
351 the  $G'_{\max}$  values of WPA systems were higher than those of the NMC or MIX systems at any  
352 concentration. This could be due to the fact that heat-induced WPA are smaller and more  
353 numerous than the casein micelles at any concentration (Andoyo et al., 2014), which increases  
354 the number of contact points (bonds) between the particles forming the gel (Anema, 2008;  
355 Van Vliet & Keetels, 1995). Heat-induced WPA also have higher surface hydrophobicity and  
356 higher pI as compared to casein micelles, hence a higher reactivity to acid gelation and longer  
357 time allowed for particle rearrangements until it reached pH 4.5 (Famelart et al., 2004).  
358 However, the theoretical  $G'_{\max}$  values, as calculated by combining 80%  $G'_{\max}$  of NMC + 20%  
359  $G'_{\max}$  of WPA, showed a lower values than the experimental  $G'_{\max}$  (Fig. 3C). Therefore, the  
360 interaction between WPA and the casein micelles in MIX systems synergistically increased  
361 the final  $G'_{\max}$ , as it increased the pH of gelation (Fig.3).

#### 362 ***3.4. Arrangement of the particles, as interpreted using rheological measurements***

363 Fig. 4A, 4B and 4C show the double-logarithmic plots of the limit of linearity ( $\gamma_0$ ) versus  
364 the total protein concentration ( $C$ ) of the WPA, NMC and MIX systems, respectively. The  
365  $\gamma_0$  data show a larger scatter than the data for  $G'$ . However, as the probability  $P$  to observe the  
366 current values of the regression coefficient was  $<0.01$  and as a regular distribution of the  
367 residuals was found, a linear regression could significantly apply to  $\log \gamma_0$  versus  $\log C$ .

368 According to Shih et al (1990), the sign of the slope (negative or positive) is indicative of  
369 distinct aggregation pathways during flocculation. Furthermore, an apparent fractal dimension  
370 ( $D_f$ ) of the WPA, NMC and MIX systems can be directly calculated from the slope of the  $\log$   
371  $G'$  versus  $\log C$  (Fig. 3C). The fractal dimension value expresses the volume occupancy by

372 the flocs: low  $D_f$  values correspond to a loose or diffuse flocs, while high  $D_f$  values correspond  
373 to compact flocs (Vetier et al., 1997). The present results show that for the WPA systems,  
374  $\gamma_0$  decreased with increasing particle concentration  $C$ . Meanwhile,  $\gamma_0$  increased with  $C$  for both  
375 the NMC and MIX systems (Fig. 4B and 4C). For a negative slope, i.e. the WPA system, the  
376 value of the backbone fractal dimension of the flocs ( $x$ ) has to be introduced. The range of the  
377  $x$  value is 1 - 1.3 (Shih et al., 1990) and therefore, in this study a maximum and a minimum  
378 value of the apparent  $D_f$  were estimated using Eq. 1, respectively. Calculated  $D_f$  values for  
379 WPA model milk gel were 1.6 - 1.7 (Fig.3C). By using eqn.3 for a positive slope of  $\log G'$   
380 versus  $\log C$ , the apparent  $D_f$  values of NMC and MIX systems were found to be 2.8 and 2.6,  
381 respectively (Fig. 3C). The values found for the casein gels (MNC and MIX) were higher than  
382 those found in previous studies on acid gels. Using light scattering measurement in diluted  
383 milk,  $D_f$  values of 1.85 – 2.44 were reported for acid casein gels (Bremer et al., 1989;  
384 Chardot, Banon, Misiuwianiec, & Hardy, 2002; Vetier et al., 1997). Values higher than 2.1  
385 can occur when the repulsive barrier is high (Mellema, Walstra, Van Opheusden, & Van  
386 Vliet, 2002), as can occur with casein micelles. The apparent  $D_f$  values therefore indicated a  
387 more compact structure of the NMC and MIX gels than that of the WPA. On the other hand,  
388 the apparent  $D_f$  value for WPA gels was lower than those determined by Alting et al. (2003)  
389 for cold-set acid WPI gels, Hagiwara et al. (1996) for heat-set BSA gel or heat-set WPI gels  
390 by Ikeda et al. (1999) (1.6 against 2.0-2.3). This deviation could arise from different proteins  
391 and gelation processes used.

392 It is interesting to notice that when casein micelles were present, i.e. in NMC and MIX  
393 systems, a similar aggregation behavior was found, as indicated by the positive slopes of  
394  $\log \gamma_0$  with  $\log C$  and by the similar  $D_f$  values, irrespective of the presence or absence of  
395 WPA. Meanwhile, it is clearly established that WPA, which do affect the final  $G'$  values of  
396 the gel (Andoyo et al., 2014; Guyomarc'h et al., 2003; Lucey & Singh, 1998), exhibited a

397 different aggregation behavior when gelled alone than when gelled in presence of the casein  
398 micelles, as shown by the negative slope of  $\log \gamma_0$  with  $\log C$  for the WPA mixture and by the  
399 lower  $D_f$  values. The reason for this may lie in the scale of the particle assembly investigated  
400 by either approach. The  $G'$  value of a mature gel typically depends also on the strength and  
401 number of links established during percolation, while it was expected from Shih et al.'s  
402 approach to probe links established during the earlier fractal flocculation.

403 Gels that incorporate casein micelles, as the MNC and MIX systems, can rearrange upon  
404 acidification due to the dissolution of the CCP at  $\text{pH} \sim 5$ . This rearrangement can allow  
405 compaction of the protein clusters (Vetier et al., 1997), thus increasing the apparent  $D_f$  of the  
406 flocs (Mellema, Heesakkers, Van Opheusden, & Van Vliet, 2000) although this might be  
407 debated (Babu, Gimel, & Nicolai, 2008). When WPA are present in the MIX, stronger  
408 hydrophobic interactions and covalent bonds may lead to a higher stiffness of the links thus  
409 reducing the possibility for particles to rearrange in more compact flocs, hence the lower  
410 apparent  $D_f$  in MIX than in NMC. Furthermore, casein assemblies have a tendency to  
411 syneresis, especially in absence but even in presence of hydrophobic whey protein aggregates  
412 (Morand et al., 2011; Schorsch, Wilkins, Jones, & Norton, 2001). Contraction of the casein  
413 gel induces local rupture and opening of pores, while casein flocs densify. Inside the flocs,  
414 bonds between casein may become shorter, stronger and numerous as material came closer to  
415 each other, while those between flocs may be stressed, stretched and weaker or less  
416 numerous. WPA themselves are made of internal SS bonds (Hoffmann & Van Mil, 1997; Jean  
417 et al., 2006; Morand et al., 2011). When they are present along the casein micelles in the MIX  
418 system, the magnitude of the force, length and number of links are probably much higher than  
419 in their absence, i.e. in the NMC system (Andoyo et al., 2014; Lakemond & Van Vliet, 2008;  
420 Walstra & Jenness, 1984). When they are acidified alone, the WPA form clusters or flocs  
421 through non-covalent interactions (Hoffmann & Van Mil, 1997). Interactions may reorganize

422 through oxidation or SH/SS exchanges provided that the local environment is adequate, for  
423 example when high concentration of sulfhydryl and disulfides are locally present (Swaisgood,  
424 2005; Guyomarc'h et al, 2014). Hence, it is suggested that it is the casein micelle fraction that  
425 actually drives the aggregation mechanism, while WPA would only affect bond strength and  
426 eventually  $G'$ . This is in line with the hypothesis that WPA particles modify the surface of the  
427 casein micelles, rendering them more prone to acid flocculation (Andoyo et al., 2014).

#### 428 *Microstructure of the gel at pH 4.5*

429 Fig. 5 shows the TEM and CLSM images of acid gels of the 3 systems at pH ~4.5. In  
430 CLSM images (inserts in Fig. 5), the white color represented the protein network and black  
431 color represent the pores of the gel. From CSLM images, increasing the protein concentration  
432 of the system led to an increase in the whiteness of the image, i.e. to less pores. Images of the  
433 NMC and MIX gels seemed very close, although they are not shown at the same  
434 concentration. In the WPA systems, the gels were fully connected through the heat-induced  
435 whey protein aggregate network. Increasing total protein concentrations in the WPA systems  
436 yielded connected network, thus leading to smaller pores (Fig. 5A, B). The formation of  
437 smaller pores in the WPA gel as compared to NMC and mixture systems may indicate more  
438 numerous connections that led to a more homogeneous gel. Confocal images of the WPA gel,  
439 made from the 5 different protein concentrations, show that the structure of gels appeared  
440 finer and with smaller pores at higher protein concentration (inserts in Fig. 5AB). As we  
441 maintained the imaging parameters constant, we point out that images at higher protein  
442 concentrations had less contrast, probably due to the fact that the fluorescent probe is more  
443 homogeneously distributed in the matrix at a higher protein concentration, and because the  
444 pore size was more or less equal to the resolution of the microscope.

445 In the NMC systems, thick strands of gel can be seen on the images. TEM images in Fig.  
446 5C showed that at low NMC concentration, the individual casein micelles particles still can be

447 seen. However, at a higher total protein concentration, the flocs of casein particles seemed to  
448 enlarge (TEM Fig. 5D). The gels of NMC system at increased NMC concentrations show  
449 smaller pore sizes, and denser, more clustered and less branched networks (insert Fig. 5C, D).  
450 In the mixture systems, branched whey protein aggregates were slightly visible (TEM insert  
451 Fig. 5A) and the casein micelles seemed intimately connected by whey protein aggregates  
452 (TEM Fig. 5EF and insert Fig. 5F). When compared with the NMC system alone, the  
453 association of heat-induced whey protein aggregates with casein micelles in the MIX system  
454 largely changed the microstructure of the gels at pH ~4.5 and at any concentration. First and  
455 very significant, the size of the casein particles seemed to be much smaller as compared to the  
456 size of the casein in the NMC systems as shown in the TEM micrograph (Fig. 5C, D, E, F).  
457 Then the structure in the MIX gel appeared more branched and flocs were less dense and  
458 more open than in the NMC gel. However, the changes of the gel microstructure at pH ~4.5 of  
459 the MIX gel were not always correlated with changes in  $G'$  values, as the 2 gels 90 g kg<sup>-1</sup>  
460 protein did show differences in their microstructures but not on their  $G'$  values (Fig. 3B).

461 Apparent  $D_f$  values of each system were also calculated from confocal and TEM images  
462 after binarization of the images. Average apparent  $D_f$  value for the 3 systems calculated with  
463 the 2 image analysis methods and with the rheological measurements method are shown in  
464 Fig. 6. The results showed a high standard deviation of the apparent  $D_f$ , measured from  
465 confocal images, which can be due to the fact that slightly different threshold values were  
466 applied on each concentration tested. Also, apparent  $D_f$  values of the WPA system could not  
467 be determined from the TEM images, probably because the WPA flocs were smaller and less  
468 contrasted than micelles one, so that no adequate thresholding could be operated.

469 Exclusive of the missing WPA value by TEM, apparent  $D_f$  values of 2.15, 2.76 and 2.74,  
470 and 2.69 and 2.64 were found for the WPA, NMC and MIX systems, respectively, using the  
471 TEM or the CLSM technique, respectively (Fig. 6). The apparent  $D_f$  values of the NMC and

MIX systems measured by image analysis agreed well with those obtained by the rheological method, the differences being lower than 5%. This indicates that image analysis is a good alternative method for the investigation of self-similarity within gels, providing that thresholding of the images is optimized using automated methods. Indeed, previous reports have shown that decreasing the grey scale thresholding parameter (i.e. increasing the number of pixels) can significantly increase the resulting  $D_f$  value (Ako, Durand, Nicolai, & Becu, 2009; Mellema et al., 2000).

### 3.6. *Limits of the self-similarity approach for dairy gels*

The concept of self-similarity has aroused a great interest in dairy science from the 80s onward, as it proposed a sensible description of protein flocculation or of fat crystallization (Alting et al., 2003; Bremer, Vanvliet, & Walstra, 1989b; Buscall et al., 1988; Hagiwara, Kumagai, Matsunaga, & Nakamura, 1997; Hagiwara et al., 1996; Marangoni et al., 2000; Mellema et al., 2000; Shih et al., 1990; Sonntag & Russel, 1987; Wu & Morbidelli, 2001). However, models are not without limitations.

Horne (1999) pointed out that fractal models fail to describe the macrostructure of acid gels of micellar casein, as they should yield gels with larger pores as the length scale increases. Alting et al. (2003) found that application of fractal models as proposed by Bremer et al. (1990) and Shih et al. (1990) to heat-induced WPI gels did not result in realistic values of the fractal dimension. They proposed that the gelation occurred with different mechanisms at certain length scales. In line with this, it could be assumed that a self-similar assembly only occurred in the suspensions at the early stages of the acid-induced aggregation, until the flocs started to come in contact, interpenetrate and eventually percolate into a gel. Therefore, the range of length scales where acid-induced self-similarity was investigated was ~0.1 to ~10  $\mu\text{m}$ , using TEM and CLSM in the presented conditions. Noteworthy, the WPA particles are themselves short fractal aggregates (Jean et al., 2006; Mahmoudi, Mehalebi, Nicolai, Durand,

497 & Riaublanc, 2007), whereas the casein micelles are seen as hierarchical homogeneous  
498 assemblies (Bouchoux, Gesan-Guiziou, Perez, & Cabane, 2010; de Kruif, Huppertz, Urban,  
499 & Petukhov, 2012). Fractality may therefore exist in WPA-containing samples below the 0.1  
500  $\mu\text{m}$  length scale (Mahmoudi et al., 2007) and it is possible that the flocculation mechanism  
501 somewhat differed from heat-induced to acid-induced aggregation.

502 According to computer simulation studies, the maximum volume fraction for which  
503 fractality can be observed over a sensible scale range is 5% for DLCA and maybe 2-3 fold  
504 that value for structures showing rearrangement (Babu et al., 2008; Rotterreau, Gimel, Nicolai,  
505 & Durand, 2004). This limitation was calculated for hard spheres and for diffusion-limited  
506 cluster aggregations. Considering their mechanism, reaction-limited assemblies are  
507 susceptible to tolerate even higher maximum volume fraction. According to Chaplain et al.  
508 (1994), as micrographs of acid- or rennet-induced dairy gels show a typical persistent size in  
509 chains of 10 particles, a limit close to 10% could be predicted for the maximal volume  
510 fraction. By analogy with the polymers gels, these authors describe the gel structure at volume  
511 fractions higher than the percolation threshold as a homogeneous packing of fractal flocs,  
512 while a scaling behavior is only observed at short range. They developed a model adapted  
513 from Bremer's, that leads to  $\log(G') \sim \log(C)^3$  at high volume fraction, that leads to a Df of 3  
514 i.e. a homogeneous gels made of fractal clusters. Our exponents of  $\log(G')$  versus  $\log(C)$   
515 were lower for gels studied in the current study (1.6-2.8). However, doubts exist on the  
516 applicability of the fractal model to as high volume fractions as those used herein. Previous  
517 groups also applied this theory to dairy systems with volume fractions in the range of those  
518 used in the present study, using either rheometry or image analysis (Bremer et al., 1989;  
519 Chaplain, Mills, & Djabourov, 1994; Hagiwara et al., 1997; Marangoni et al., 2000; Vetier,  
520 Banon, Ramet, & Hardy, 2000; Zhong, Daubert, & Velev, 2004, 2007; Ikeda et al., 1999;  
521 Pugnali et al., 2005; Torres et al., 2012). Many thermo-induced gels or flocs of whey

522 proteins at large volume fractions are also reported to be of fractal nature (Hagiwara,  
523 Kumagai, & Matsunaga, 1997; Hagiwara, Kumagai, & Nakamura, 1998; Pouzot, Nicolai,  
524 Benyahia, & Durand, 2006; Stading, Langton, & Hermansson, 1993; Verheul & Roefs, 1998).  
525 In their study, Ako et al. (2009) investigated the structure of  $100 \text{ g L}^{-1}$   $\beta$ -lactoglobulin heat-set  
526 gels in 0.15-2 M NaCl, using CLSM and image analysis.

527 They found that the normalized pair correlation function  $g(r)$  did not show a power law  
528 dependence on  $r$  that would be expected for a fractal structure. Instead,  $g(r)$  could be  
529 described by a stretched exponential decay. Nevertheless, an apparent fractal dimension could  
530 be derived using the box counting method. This finding raises the question of the validity of  
531 the large number of studies that aimed at estimating fractal dimension in acid dairy gels at  
532 concentrations  $> 15 \text{ g L}^{-1}$ . Another interesting issue in this debate would be to agree on the  
533 calculation of volume fraction of hydrated and porous particles like the casein micelles or the  
534 WPA, which are not exactly hard spheres.

535 Another limitation of the self-similarity concept is that one should find a compromise  
536 between extending the range of explored length scales through decreasing the protein  
537 concentration (and hence, through postponing percolation) and having samples that can stand  
538 rheological measurements or preparation for electron microscopy without breakage or phase  
539 separation. Hence, if low volume fractions are required to apply the fractal model, one may be  
540 limited by the sample itself. Mehalebi et al (2007) could observe heat-induced fractal  
541 structures formed at high volume fraction, only after large dilution of the samples to disperse  
542 the interpenetrating flocs.

543 Finally, a third limitation to the fractal theory is that one should assume that the particle  
544 do not experience larger rearrangement than shifts in relative positions and may be slight  
545 change in volume. Structural rearrangement occurred when casein micelles was present in the  
546 systems, as evidenced by the local maximum of  $\tan \delta$  at pH  $\sim 5.0$  (Fig.1D and 1F), which may

547 affect rheological measurements parameters such as  $G'_{\max}$  and  $\gamma_0$ , therefore could implies to  
548 the applicability of the fractal models.

549 In conclusion, the rheological properties and microstructure of 3 model systems, namely  
550 NMC, WPA and MIX system, were investigated for a certain range of concentrations. Results  
551 show that increasing the protein concentration for the 3 systems promoted a faster gelation,  
552 led to higher moduli and to gels with smaller pore sizes, which is due to the increase in the  
553 number of particles and consequently probably in the number of potential bonds between  
554 them and to the reduction in the distances between colloids. Replacing 20 % of NMC by  
555 WPA, as in MIX systems, increased the moduli of the acid gels as long as the protein  
556 concentrations was  $< 90 \text{ g kg}^{-1}$  and increased their pH of gelation as compared to pure NMC  
557 gels. Although limitations existed, the model of Shih et al. (1990) indicated that the  
558 aggregation behavior of the MIX system was similar to that of the NMC, and not of the WPA.  
559 This result showed that the casein micelles directed the aggregation pathway wherever they  
560 were present in the samples. On the other hand, WPA only seemed to impact on the amplitude  
561 of the elastic modulus of the resulting gel, probably through affecting the strength of the  
562 involved bonds. Further research is needed to be able to confirm these findings in conditions  
563 where the scaling theory would fully apply.

#### 564 **Acknowledgements**

565 We wish to thank MT LAVAUULT from the Microscopy Rennes Imaging Center of SFR  
566 BIOSIT, Université de Rennes 1 France for her expertise in TEM experiments. This work was  
567 financially supported by the Directorate General of Higher Education (DGHE) of the Ministry  
568 of Education and Culture of the Republic of Indonesia, as part of the DGHE scholarship  
569 overseas program.

#### 570 **References**

- 571 Ako, K., Durand, D., Nicolai, T., & Becu, L. (2009). Quantitative analysis of confocal laser  
572 scanning microscopy images of heat-set globular protein gels. *Food Hydrocolloids*,  
573 23(4), 1111–1119.
- 574 Alexander, M., Corredig, M., & Dalgleish, D. G. (2006). Diffusing wave spectroscopy of  
575 gelling food systems: The importance of the photon transport mean free path ( $l^*$ )  
576 parameter. *Food Hydrocolloids*, 20, 325–331.
- 577 Alexander, M., & Dalgleish, D. G. (2005). Interactions between denatured milk serum  
578 proteins and casein micelles studied by diffusing wave spectroscopy. *Langmuir*,  
579 21(24), 11380–11386.
- 580 Alting, A. C., Hamer, R. J., de Kruif, C. G., & Visschers, R. W. (2003). Cold-set globular  
581 protein gels: interactions structure and rheology as a function of protein concentration.  
582 *Journal of Agricultural and Food Chemistry*, 51(10), 3150–3156.
- 583 Andoyo, R., Guyomarc'h, F., Cauty, C., & Famelart, M.-H. (2014). Model mixtures evidence  
584 the respective roles of whey protein particles and casein micelles during acid gelation.  
585 *Food Hydrocolloids*, 37, 203–212.
- 586 Anema, S. (2009). Role of colloidal calcium phosphate in the acid gelation properties of  
587 heated skim milk. *Food Chemistry*, 114, 161–167.
- 588 Anema, S. G. (2008). Effect of milk solids concentration on the gels formed by the  
589 acidification of heated pH-adjusted skim milk. *Food Chemistry*, 108(1), 110–118.
- 590 Awad, T. S., Rogers, M. A., & Marangoni, A. G. (2004). Scaling behavior of the elastic  
591 modulus in colloidal networks of fat crystals. *The Journal of Physical Chemistry B*,  
592 108(1), 171–179.
- 593 Babu, S., Gimel, J. C., & Nicolai, T. (2008). Diffusion limited cluster aggregation with  
594 irreversible slippery bonds. *The European Physical Journal E*, 27(3), 297–308.

- 595 Bertoluzzo, M. G., Bertoluzzo, S. M., Luisetti, J. A., & Gatti, C. A. (1998). A bidimensional  
596 simulation of particle cluster aggregation with variable active sites particles. *Colloid*  
597 *and Polymer Science*, 276(5), 443–445.
- 598 Bi, C., Li, D., Wang, L., & Adhikari, B. (2013). Viscoelastic properties and fractal analysis of  
599 acid-induced SPI gels at different ionic strength. *Carbohydrate Polymers*, 92(1), 98–  
600 105.
- 601 Bouchoux, A., Gesan-Guiziou, G., Perez, J., & Cabane, B. (2010). How to squeeze a sponge  
602 casein micelles under osmotic stress, a SAXS study. *Biophysical Journal*, 99(11),  
603 3754–3762.
- 604 Bremer, L. G. B., Bijsterbosch, B. H., Schrijvers, R., Van Vliet, T., & Walstra, P. (1990). On  
605 the fractal nature of the structure of acid casein gels. *Colloids and Surfaces*, 51, 159–  
606 170.
- 607 Bremer, L. G. B., Vanvliet, T., & Walstra, P. (1989a). Theoretical and experimental-study of  
608 the fractal nature of the structure of casein gels. *Journal of the Chemical Society-*  
609 *Faraday Transactions I*, 85, 3359–3372.
- 610 Buscall, R., Mills, P., Goodwin, J., & Lawson, D. (1988). Scaling behavior of the rheology of  
611 aggregate networks formed from colloidal particles. *Journal of the Chemical Society-*  
612 *Faraday Transactions I*, 84, 4249–4260.
- 613 Chaplain, V., Mills, P., & Djabourov, M. (1994). Elastic properties of networks of fractal  
614 clusters. *Colloid and Polymer Science*, 272(8), 991–999.
- 615 Chardot, V., Banon, S., Misiuwianiec, M., & Hardy, J. (2002). Growth kinetics and fractal  
616 dimensions of casein particles during acidification. *Journal of Dairy Science*, 85, 8–  
617 14.

- 618 Dalgleish, D. G. (2011). On the structural models of bovine casein micelles-review and  
619 possible improvements. *Soft Matter*, 7(6), 2265–2272.
- 620 De Kruif, C. G. (1999). Casein micelle interactions. *International Dairy Journal*, 9, 183–188.
- 621 De Kruif, C. G., Huppertz, T., Urban, V. S., & Petukhov, A. V. (2012). Casein micelles and  
622 their internal structure. *Advances in Colloid and Interface Science*, 171, 36–52.
- 623 De Kruif, C., & Huppertz, T. (2012). Casein micelles: size distribution in milks from  
624 individual cows. *Journal of Agricultural and Food Chemistry*, 60(18), 4649–4655.
- 625 Donato, L., Alexander, M., & Dalgleish, D. G. (2007). Acid gelation in heated and unheated  
626 milks: interactions between serum protein complexes and the surfaces of casein  
627 micelles. *Journal of Agricultural and Food Chemistry*, 55(10), 4160–4168.
- 628 Donato, L., & Guyomarc'h, F. (2009). Formation and properties of the whey protein/ $\kappa$ -casein  
629 complexes in heated skim milk - a review. *Dairy Science and Technology*, 89, 3–29.
- 630 Donato, L., Guyomarc'h, F., Amiot, S., & Dalgleish, D. G. (2007). Formation of whey  
631 protein/ $\kappa$ -casein complexes in heated milk: Preferential reaction of whey protein with  
632  $\kappa$ -casein in the casein micelles. *International Dairy Journal*, 17(10), 1161–1167.
- 633 Dong, Y. J., Wang, Y. L., & Feng, J. (2011). Rheological and fractal characteristics of  
634 unconditioned and conditioned water treatment residuals. *Water Research*, 45(13),  
635 3871–3882.
- 636 Eissa, A. S., & Khan, S. A. (2005). Acid-induced gelation of enzymatically modified,  
637 preheated whey proteins. *Journal of Agricultural and Food Chemistry*, 53(12), 5010–  
638 5017.

- 639 Famelart, M. H., Lepasant, F., Gaucheron, F., Le Graet, Y., & Schuck, P. (1996). pH-Induced  
640 physicochemical modifications of native phosphocaseinate suspensions: Influence of  
641 aqueous phase. *Le Lait*, 76, 445–460.
- 642 Famelart, M. H., Tomazewski, J., Piot, M., & Pezennec, S. (2004). Comprehensive study of  
643 acid gelation of heated milk with model protein systems. *International Dairy Journal*,  
644 14, 313–321.
- 645 Fox, P. F., & Brodkorb, A. (2008). The casein micelle: Historical aspects, current concepts  
646 and significance. *International Dairy Journal*, 18(7), 677–684.
- 647 Genovese, D. B. (2012). Shear rheology of hard-sphere, dispersed, and aggregated  
648 suspensions, and filler-matrix composites. *Advances in Colloid and Interface Science*,  
649 171, 1–16.
- 650 Guyomarc'h, F., Famelart, M.-H., Henry, G., Gulzar, M., Leonil, J., Hamon, P., Croguennec,  
651 T. (2014). Current ways to modify the structure of whey proteins for specific  
652 functionalities—a review. *Dairy Science & Technology*, 1–20.
- 653 Guyomarc'h, F., Jemin, M., Le Tilly, V., Madec, M. N., & Famelart, M. H. (2009). Role of  
654 the heat-induced whey protein/ $\kappa$ -casein complexes in the formation of acid milk gels:  
655 a kinetic study using rheology and confocal microscopy. The 5th International  
656 Symposium on Food Rheology and Structure.
- 657 Guyomarc'h, F., Queguiner, C., Law, A. J. R., Horne, D. S., & Dalgleish, D. G. (2003). Role  
658 of the soluble and micelle-bound heat-induced protein aggregates on network  
659 formation in acid skim milk gels. *Journal of Agricultural and Food Chemistry*, 51(26),  
660 7743–7750.
- 661 Guyomarc'h, F., Renan, M., Chatriot, M., Gamarre, V., & Famelart, M. H. (2007). Acid  
662 gelation properties of heated skim milk as a result of enzymatically induced changes

- 663 in the micelle/serum distribution of the whey protein/ $\kappa$ -casein aggregates. *Journal of*  
664 *Agricultural and Food Chemistry*, 55(26), 10986–10993.
- 665 Hagiwara, T., Kumagai, H., & Matsunaga, T. (1997). Fractal analysis of the elasticity of BSA  
666 and  $\beta$ -lactoglobulin gels. *Journal of Agricultural and Food Chemistry*, 45(10), 3807–  
667 3812.
- 668 Hagiwara, T., Kumagai, H., Matsunaga, T., & Nakamura, K. (1997). Analysis of aggregate  
669 structure in food protein gels with the concept of fractal. *Bioscience Biotechnology &*  
670 *Biochemistry*, 61, 1663–1667.
- 671 Hagiwara, T., Kumagai, H., & Nakamura, K. (1996). Fractal analysis of aggregates formed by  
672 heating dilute BSA solutions using light scattering methods. *Bioscience Biotechnology*  
673 *and Biochemistry*, 60(11), 1757–1763.
- 674 Hagiwara, T., Kumagai, H., & Nakamura, K. (1998). Fractal analysis of aggregates in heat-  
675 induced BSA gels. *Food Hydrocolloids*, 12(1), 29–36.
- 676 Hoffmann, M. A. M., & Vanmil, P. J. J. M. (1997). Heat-induced aggregation of  $\beta$ -  
677 lactoglobulin: role of the free thiol group and disulfide bonds. *Journal of Agricultural*  
678 *and Food Chemistry*, 45(8), 2942–2948.
- 679 Holt, C. (1992). Structure and stability of bovine casein micelle. *Advances in Protein*  
680 *Chemistry*, 43:63-151, 63–151.
- 681 Horne, D. S. (1998). Casein interactions: casting light on the black boxes, the structure in  
682 dairy products. *International Dairy Journal*, 8, 171–177.
- 683 Horne, D. S. (1999). Formation and structure of acidified milk gels. *International Dairy*  
684 *Journal*, 9, 261–268.

- 685 Horne, D. S. (2001). Factors influencing acid-induced gelation of skim milk. In E. Dickinson  
686 & R. Miller (Eds.), *Food colloids: fundamentals of formulation* (pp. 345–351).  
687 Cambridge UK: Royal Society of Chemistry.
- 688 Ikeda, S., Foegeding, E. A., & Hagiwara, T. (1999). Rheological study on the fractal nature of  
689 the protein gel structure. *Langmuir*, *15*(25), 8584–8589.
- 690 Jean, K., Renan, M., Famelart, M. H., & Guyomarc'h, F. (2006). Structure and surface  
691 properties of the serum heat-induced protein aggregates isolated from heated skim  
692 milk. *International Dairy Journal*, *16*, 303–315.
- 693 Kalab, M. (1981). Electron microscopy of milk products : A review of techniques. *Scanning*  
694 *Electron Microscopy*, *3*, 453–472.
- 695 Kaye, B. H. (1994). *A random walk through fractal dimensions*. Weinheim; New York: VCH.
- 696 Kuhn, K. R., Cavallieri, Â. L. F., & Da Cunha, R. L. (2010). Cold-set whey protein gels  
697 induced by calcium or sodium salt addition. *International Journal of Food Science &*  
698 *Technology*, *45*(2), 348–357.
- 699 Lakemond, C. M. M., & Van Vliet, T. (2008). Rheological properties of acid skim milk gels  
700 as affected by the spatial distribution of the structural elements and the interaction  
701 forces between them. *International Dairy Journal*, *18*(5), 585–593.
- 702 Lucey, J. A. (2002). Formation and physical properties of milk protein gels. *Journal of Dairy*  
703 *Science*, *85*, 281–294.
- 704 Lucey, J. A., & Singh, H. (1998). Formation and physical properties of acid milk gels: a  
705 review. *Food Research International*, *30*(7), 529–542.
- 706 Mahmoudi, N., Mehalebi, S., Nicolai, T., Durand, D., & Riaublanc, A. (2007). Light-  
707 scattering study of the structure of aggregates and gels formed by heat-denatured whey

- 708 protein isolate and  $\beta$ -lactoglobulin at neutral pH. *Journal of Agricultural and Food*  
709 *Chemistry*, 55(8), 3104–3111.
- 710 Marangoni, A. G., Barbut, S., McGauley, S. E., Marcone, M., & Narine, S. S. (2000). On the  
711 structure of particulate gels - the case of salt-induced cold gelation of heat-denatured  
712 whey protein isolate. *Food Hydrocolloids*, 14(1), 61–74.
- 713 Mellema, M., Heesakkers, J. W. M., Van Opheusden, J. H. J., & Van Vliet, T. (2000).  
714 Structure and scaling behavior of aging rennet-induced casein gels examined by  
715 confocal microscopy and permeametry. *Langmuir*, 16(17), 6847–6854.
- 716 Mellema, M., Walstra, P., Van Opheusden, J. H. J., & Van Vliet, T. (2002). Effects of  
717 structural rearrangements on the rheology of rennet-induced casein particle gels.  
718 *Advances in Colloid and Interface Science*, 98(1), 25–50.
- 719 Morand, M., Dekkari, A., Guyomarc'h, F., & Famelart, M. H. (2012). Increasing the  
720 hydrophobicity of the heat-induced whey protein complexes improves the acid  
721 gelation of skim milk. *International Dairy Journal*, 25(2), 103–111.
- 722 Morand, M., Guyomarc'h, F., Legland, D., & Famelart, M. H. (2012). Changing the  
723 isoelectric point of the heat-induced whey protein complexes affects the acid gelation  
724 of skim milk. *International Dairy Journal*, 23, 9–17.
- 725 Morand, M., Guyomarc'h, F., Pezennec, S., & Famelart, M. H. (2011). On how  $\kappa$ -casein  
726 affects the interactions between the heat-induced whey protein/ $\kappa$ -casein complexes  
727 and the casein micelles during the acid gelation of skim milk. *International Dairy*  
728 *Journal*, 21, 670–678.
- 729 Nair, P. K., Dalgleish, D. G., & Corredig, M. (2013). Colloidal properties of concentrated  
730 heated milk. *Soft Matter*, 9(14), 3815–3824.

- 731 Noebel, S., Weidendorfer, K., & Hinrichs, J. (2012). Apparent voluminosity of casein  
732 micelles determined by rheometry. *Journal of Colloid and Interface Science*, 386,  
733 174–180.
- 734 Ozcan-Yilsay, T., Lee, W. J., Horne, D., & Lucey, J. A. (2007). Effect of trisodium citrate on  
735 rheological and physical properties and microstructure of yogurt. *Journal of Dairy*  
736 *Science*, 90(4), 1644–1652.
- 737 Panouillé, M., Durand, D., Nicolai, T., Larquet, E., & Boisset, N. (2005). Aggregation and  
738 gelation of micellar casein particles. *Journal of Colloid and Interface Science*, 287(1),  
739 85–93.
- 740 Parris, N., Anama, S. G., Singh, H., & Creamer, L. K. (1993). Aggregation of whey proteins  
741 in heated sweet whey. *Journal of Agricultural and Food Chemistry*, 41(3), 460–464.
- 742 Parris, N., Hollar, C. M., Hsieh, A., & Cockley, K. D. (1997). Thermal stability of whey  
743 protein concentrate mixtures: aggregates formation. *Journal of Dairy Science*, 80, 19–  
744 28.
- 745 Pawley, J. (2010). *Handbook of Biological Confocal Microscopy*. Springer Science &  
746 Business Media.
- 747 Pouzot, M., Nicolai, T., Benyahia, L., & Durand, D. (2006). Strain hardening and fracture of  
748 heat-set fractal globular protein gels. *Journal of Colloid and Interface Science*, 293(2),  
749 376–383.
- 750 Pugnali, L. A., Matia-Merino, L., & Dickinson, E. (2005). Microstructure of acid-induced  
751 caseinate gels containing sucrose: Quantification from confocal microscopy and image  
752 analysis. *Colloids and Surfaces B: Biointerfaces*, 42(3-4), 211–217.

- 753 Rottureau, M., Gimel, J. C., Nicolai, T., & Durand, D. (2004). Monte Carlo simulation of  
754 particle aggregation and gelation: II. Pair correlation function and structure factor.  
755 *European Physical Journal E*, 15(2), 141–148.
- 756 Schorsch, C., Wilkins, D. K., Jones, M. ., & Norton, I. T. (2001). Gelation of casein-whey  
757 mixtures: effects of heating whey proteins alone or in the presence of casein micelles.  
758 *Journal of Dairy Research*, 68, 471–481.
- 759 Schuck, P., Piot, M., Mejean, S., Le Graet, Y., Fauquant, J., Brulé, G., & Maubois, J. L.  
760 (1994). Déhydratation par atomisation de phosphocaséinate natif obtenu par  
761 microfiltration sur membrane. *Le Lait*, 74, 375-388.
- 762 Shih, W. H., Shih, W. Y., Kim, S. I., Liu, J., & Aksay, I. A. (1990). Scaling Behavior of the  
763 Elastic Properties of Colloidal Gels. *Physical Review A*, 42(8), 4772–4779.
- 764 Singh, H., & Creamer, L. K. (1991). Aggregation and dissociation of milk protein complexes  
765 in heated reconstituted concentrated skim milks. *Journal of Food Science*, 56, 238–  
766 246.
- 767 Sonntag, R., & Russel, W. (1987). Elastic Properties of Flocculated Networks. *Journal of*  
768 *Colloid and Interface Science*, 116(2), 485–489.
- 769 Stading, M., Langton, M., & Hermansson, A. M. (1993). Microstructure and rheological  
770 behavior of particulate  $\beta$ -lactoglobuline gels. *Food Hydrocolloids*, 7, 195–212.
- 771 Swaisgood, H. E. (2005). The importance of disulfide bridging. *Biotechnology Advances*,  
772 23(1), 71–73.
- 773 Torres, I. C., Amigo Rubio, J. M., & Ipsen, R. (2012). Using fractal image analysis to  
774 characterize microstructure of low-fat stirred yoghurt manufactured with  
775 microparticulated whey protein. *Journal of Food Engineering*, 109(4), 721–729.

- 776 Van Hooydonk, A. C. M., Hagedoorn, H. G., & Boerrigter, I. J. (1986). pH-induced physico-  
777 chemical changes of casein micelles in milk and their effect on renneting. 1. Effect of  
778 acidification on physico-chemical properties. *Netherlands Milk and Dairy Journal*,  
779 *40*(2/3), 281–296.
- 780 Van Vliet, T., & Keetels, C. J. A. M. (1995). Effect of preheating of milk on the structure of  
781 acidified milk gels. *Netherlands Milk and Dairy Journal*, *49*, 27–35.
- 782 Van Vliet, T., Roefs, S. P. F. M., Zoon, P., & Walstra, P. (1989). Rheological properties of  
783 casein gels. *Journal of Dairy Research*, *56*, 529–534.
- 784 Vasbinder, A. J., van de Velde, F., & de Kruif, C. G. (2004). Gelation of casein-whey protein  
785 mixtures. *Journal of Dairy Science*, *87*, 1167–1176.
- 786 Verheul, M., & Roefs, S. P. F. M. (1998). Structure of whey protein gels, studied by  
787 permeability, scanning electron microscopy and rheology. *Food Hydrocolloids*, *12*(1),  
788 17–24.
- 789 Vetier, N., Banon, S., Ramet, J. P., & Hardy, J. (2000). Casein micelle solvation and fractal  
790 structure of milk aggregates and gels. *Lait*, *80*(2), 237–246.
- 791 Vetier, N., Desobry-Banon, S., Ould-Eleya, M. M., & Hardy, J. (1997). Effect of temperature  
792 and acification rate on the fractal dimension of acidified casein aggregates. *Journal of*  
793 *Dairy Science*, *80*, 3131–3166.
- 794 Walstra, P., & Jenness, R. (1984). *Dairy chemistry and physics*. New York: John Wiley &  
795 Sons.
- 796 Wang, Y., Lu, J., Du, B., Shi, B., & Wang, D. (2009). Fractal analysis of polyferric chloride-  
797 humic acid (PFC-HA) flocs in different topological spaces. *Journal of Environmental*  
798 *Sciences*, *21*(1), 41–48.

799 Wu, H., & Morbidelli, M. (2001). A Model Relating Structure of Colloidal Gels to Their  
800 Elastic Properties. *Langmuir*, 17(4), 1030–1036.

801 Zhong, Q., Daubert, C. R., & Velev, O. D. (2004). Cooling Effects on a Model Rennet Casein  
802 Gel System: Part I. Rheological Characterization. *Langmuir*, 20(18), 7399–7405.

803 Zhong, Q., Daubert, C. R., & Velev, O. D. (2007). Physicochemical variables affecting the  
804 rheology and microstructure of rennet casein gels. *Journal of Agricultural and Food*  
805 *Chemistry*, 55(7), 2688–2697.

806

**Figure caption**

**Fig. 1.** Storage modulus ( $G'$ ) on a log scale and  $\tan \delta$  as a function of pH recorded during acidification at 35 °C of whey protein aggregates (WPA) systems (A and B), native micellar casein (NMC) systems (C and D) and the mixture (MIX) of 80% NMC and 20% of WPA systems (E and F) at different protein concentrations. In A-B, black is 13.42 g kg<sup>-1</sup>, blue is 26.85 g kg<sup>-1</sup>, purple is 40.27 g kg<sup>-1</sup>, red is 53.69 g kg<sup>-1</sup>, and green is 62.64 g kg<sup>-1</sup> protein. In C-D, black is 42.16 g kg<sup>-1</sup>, blue is 56.22 g kg<sup>-1</sup>, purple 70.27 g kg<sup>-1</sup>, red is 84.33 g kg<sup>-1</sup> and green is 98.38 g kg<sup>-1</sup> protein. In E-F, black is 13.92 g kg<sup>-1</sup>, blue is 27.86 g kg<sup>-1</sup>, purple is 41.78 g kg<sup>-1</sup>, red is 55.71 g kg<sup>-1</sup>, brown is 69.64 g kg<sup>-1</sup> and green is 83.57 g kg<sup>-1</sup> protein. Full and dashed lines in the same color indicate repetitions. Arrows indicate the direction of the protein concentrations increase.

**Fig. 2.** pH at  $\tan \delta_{\max}$  as a function of casein concentration in native micellar casein (NMC) systems (o) and in the mixture system (MIX) of 80% NMC and 20% of WPA (●). The line drawn is of the form of the equation of Debye Huckel.

**Fig. 3.** pH of gelation of whey protein aggregates (WPA) systems (O), native micellar casein (NMC) systems (◇) and mixture (MIX) systems (△) at different protein concentrations (A), electrophoretic mobility of WPA (O) and NMC (◇) (B) and double log storage modulus at pH 4.5,  $G'_{\max}$  as a function of protein concentration (C) of WPA systems (O), NMC systems (◇) and MIX systems (△). Vertical bars indicate the standard deviation. The theoretical values of  $G'_{\max}$  and pH of gelation for the mixture systems were calculated by using the content in each protein and their own  $G'$  and pH of gelation, respectively (■).  $D_f$  is the fractal dimension value of each system, calculated from the slope of double-log  $G'_{\max}$  versus  $C$ .

**Fig. 4.** Log-log plot of the limit of linearity ( $\gamma$ ) versus the protein concentration ( $C$ ) of the WPA systems (A), NMC system (B) and MIX systems (C). Inserted in panel B is an example

of estimation of the limit of linearity ( $\gamma_0$ ) from shear stress - strain curve of the model system.

The linear regression is drawn to show  $\gamma_0$  value as the strain above which the slope of the stress versus strain curve decreased of 5% from its maximal value.

**Fig. 5.** Transmission electron micrographs and confocal images of gels from the three different systems and at two different total protein concentrations: WPA (A, B); NMC (C, D); MIX (E, F); low concentration (A, C, E) and high concentration (B, D, F). TEM at higher magnification (inserts B, F).

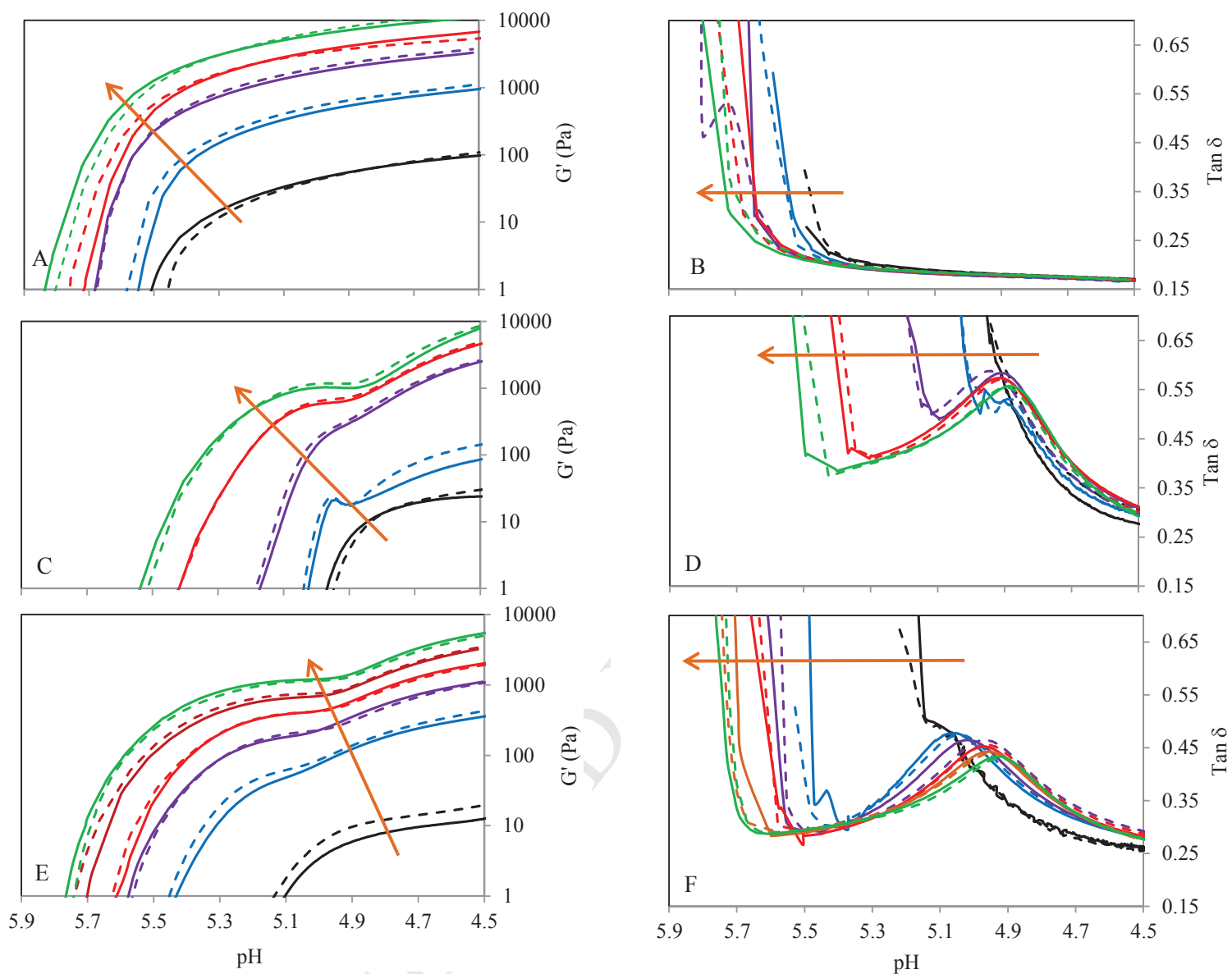
**Fig. 6.** Fractal dimension ( $D_f$ ) of the different systems measured with different methods. Vertical bars represent the standard deviation from images analyzed at different concentrations.

1 **Table captions**2 **Table 1**

3 Composition of the model milk protein systems and GDL concentrations used to reach pH 4.5  
 4 in 6 h at 35°C. The 3 systems are the native micellar casein system (NMC), the whey protein  
 5 aggregate system (WPA) and the mixture system (MIX) of 80% NMC and 20% of WPA.

| Model system | Casein<br>(g kg <sup>-1</sup> ) | Whey proteins<br>(g kg <sup>-1</sup> ) | Total protein concentration<br>(g kg <sup>-1</sup> ) | GDL Conc.<br>(g kg <sup>-1</sup> ) |
|--------------|---------------------------------|--|--|------------------------------------|
| WPA15        | -                               | 13.42                                  | 13.42  | 5.84                               |
| WPA30        | -                               | 26.85                                  | 26.85  | 7.69                               |
| WPA45        | -                               | 40.27                                  | 40.27  | 9.54                               |
| WPA60        | -                               | 53.69                                  | 53.69  | 11.39                              |
| WPA70        | -                               | 62.64                                  | 62.64  | 12.63                              |
| NMC45        | 42.16                           | -                                      | 42.16  | 18.74                              |
| NMC60        | 56.22                           | -                                      | 56.22  | 23.06                              |
| NMC75        | 70.27                           | -                                      | 70.27  | 27.39                              |
| NMC90        | 84.33                           | -                                      | 84.33  | 31.71                              |
| NMC105       | 98.38                           | -                                      | 98.38  | 36.03                              |
| MIX15        | 11.24                           | 2.68                                   | 13.92  | 8.71                               |
| MIX30        | 22.49                           | 5.37                                   | 27.86  | 12.55                              |
| MIX45        | 33.73                           | 8.05                                   | 41.78  | 16.39                              |
| MIX60        | 44.97                           | 10.74                                  | 55.71  | 20.23                              |
| MIX75        | 56.22                           | 13.42                                  | 69.64  | 24.06                              |
| MIX90        | 67.46                           | 16.11                                  | 83.57  | 27.90                              |

6

**Fig. 1.**

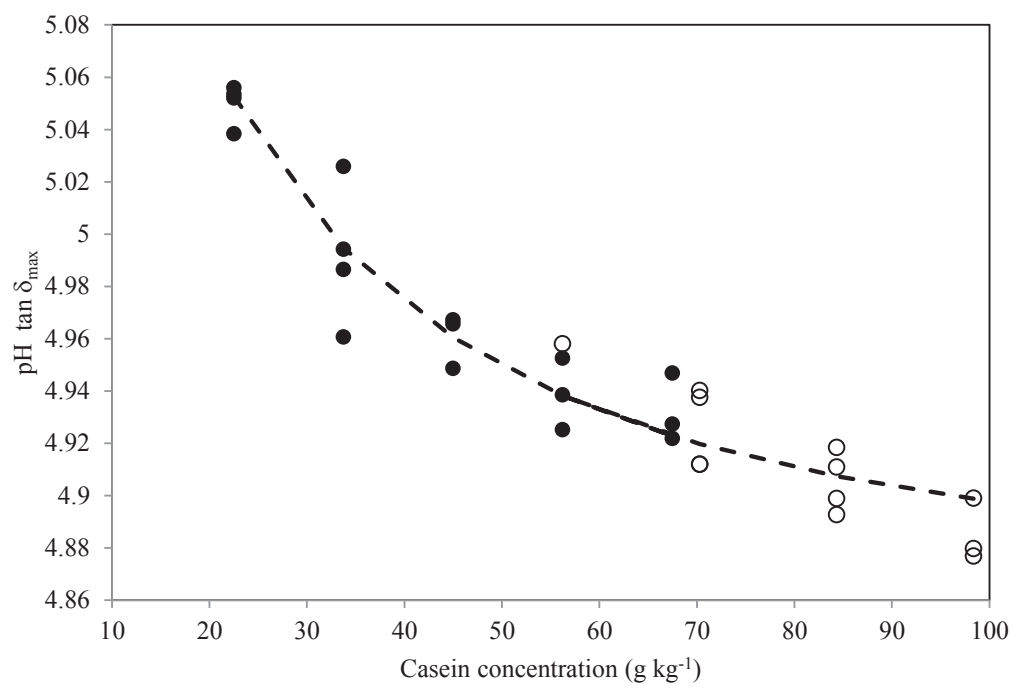


Fig. 2.

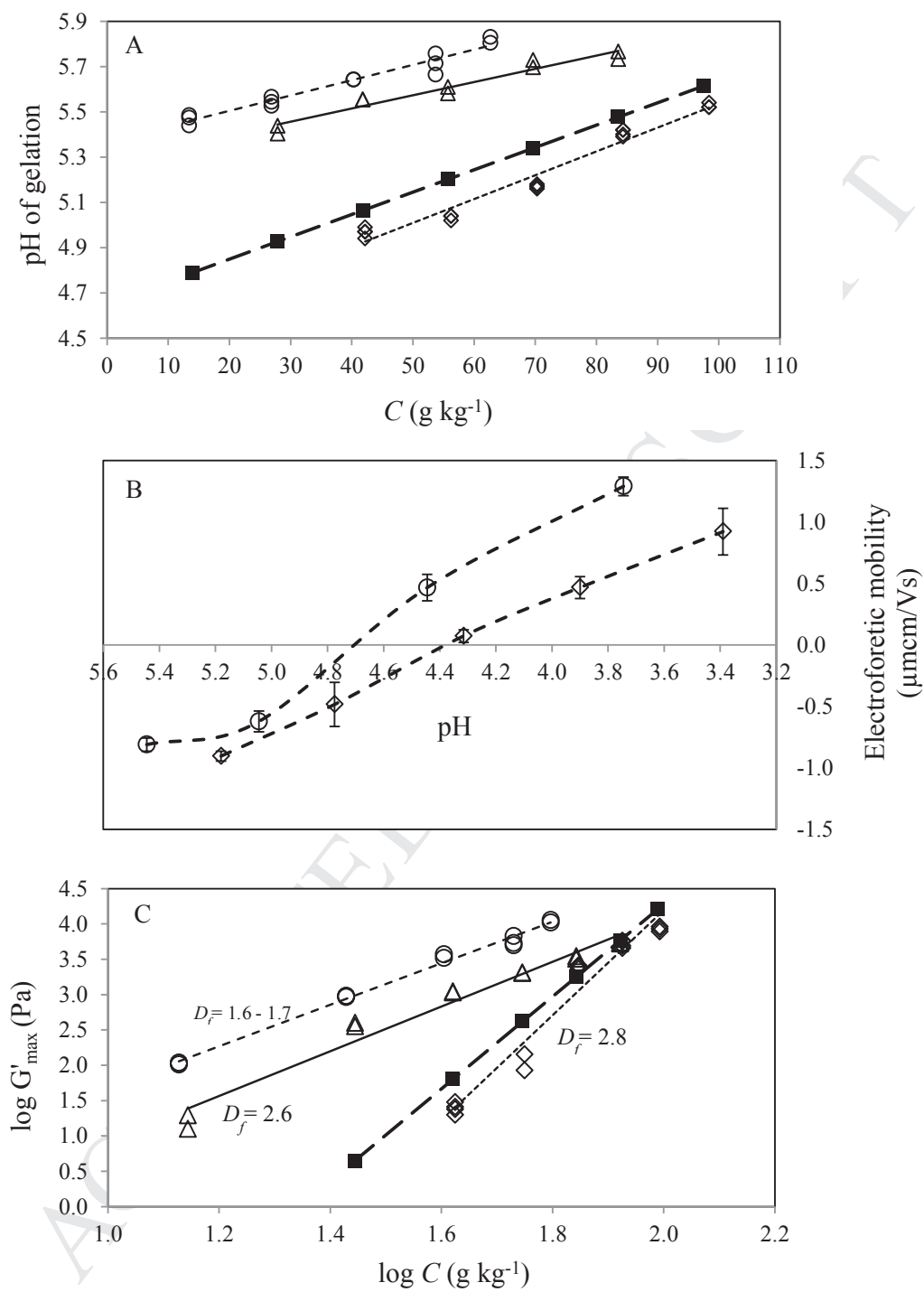


Fig. 3.

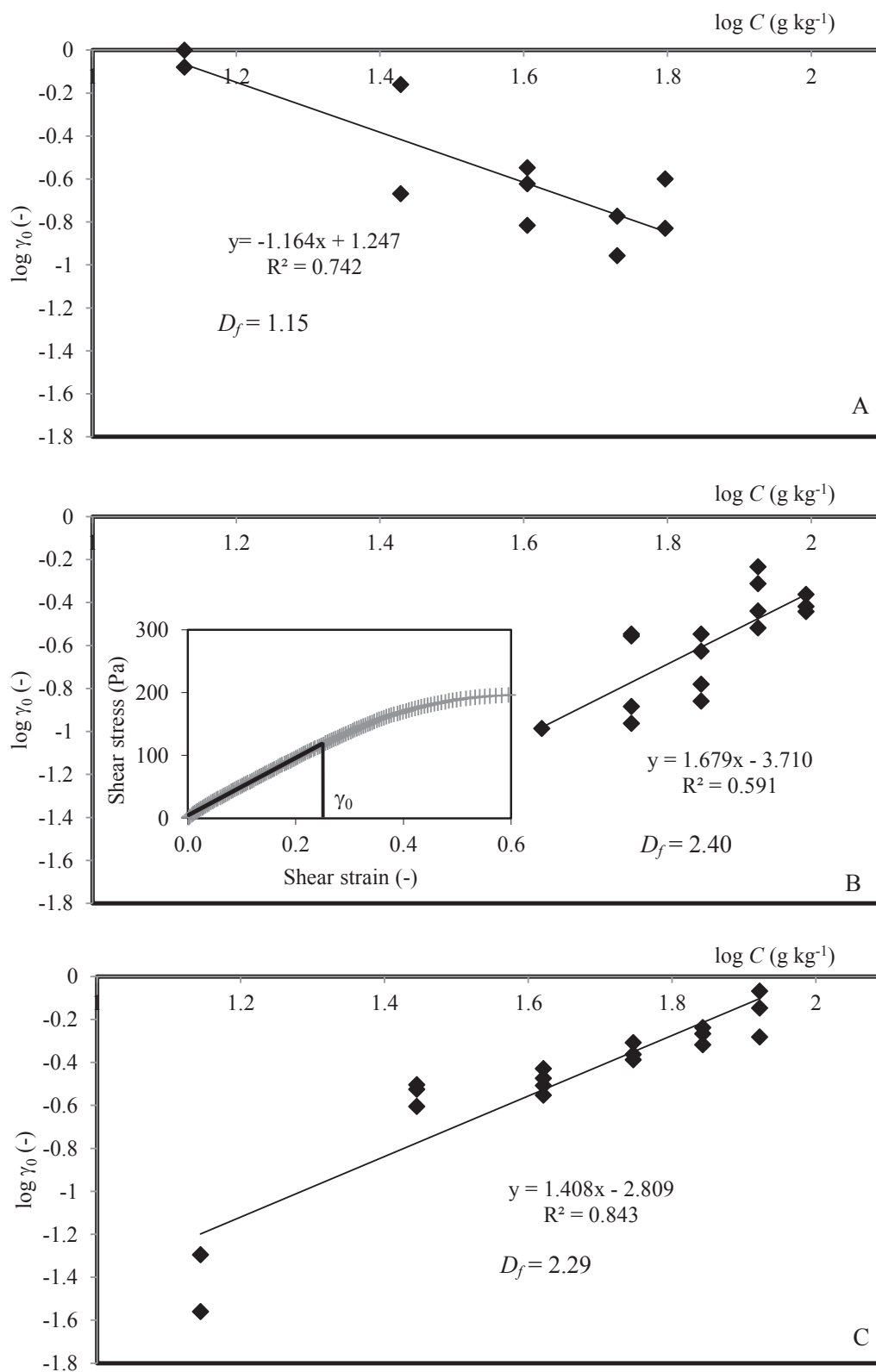
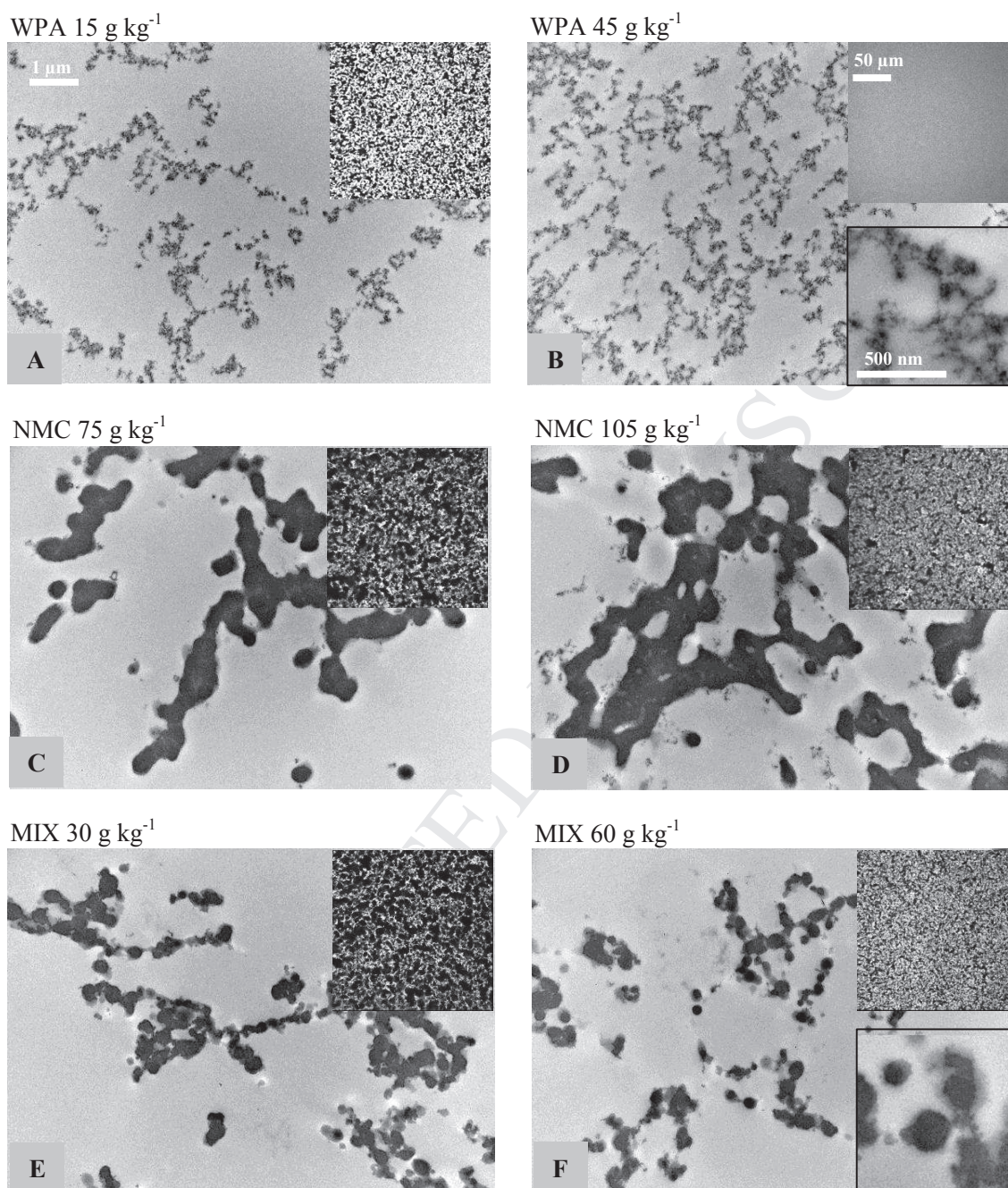
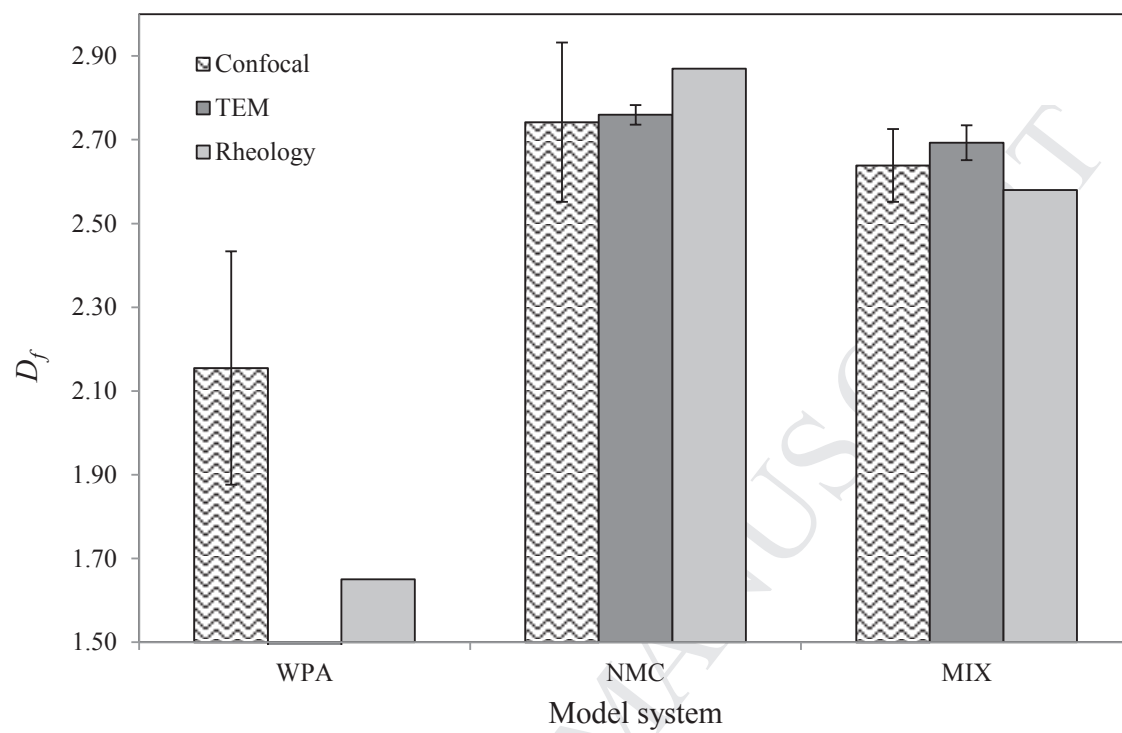


Fig. 4.

**Fig. 5.**

**Fig. 6.**

## Highlights

- Acid gels were made from casein micelles (NMC) and whey protein aggregates (WPA)
- Acid gels were made from 80/20 mixtures of NMC and WPA, respectively
- Fractal dimension ( $D_f$ ) of gel flocs were determined by rheology and image analysis
- Replacement of 20% NMC by WPA hardly changes the  $D_f$  value of the flocs
- Aggregation in the NMC and MIX mixtures was driven by the casein micelles